scientific reports

Check for updates

OPEN

Bacterial acidic agents-assisted multi-elemental (Ni, Co, and Li) leaching of used lithium-ion batteries at high pulp densities

Ahmad Heydarian[1], Farzane Vakilchap[1], Seyedeh Neda Mousavi[1] & Seyyed Mohammad Mousavi[1,2]✉

Accumulating used lithium-ion battery cathodes and associated environmental concerns necessitate efficient recycling strategies. Biohydrometallurgical processes often face challenges at high pulp densities due to microbial inhibition and substrate limitations, particularly sulfur availability, which is crucial for bacterial acidic agent production. This study introduces a breakthrough spent-medium bioleaching approach optimized for high-pulp-density conditions. We systematically addressed key challenges, including bacterial inhibition, sulfuric acid optimization, and its impact on critical metal dissolution. Using response surface methodology, we optimized sulfur dosage, inoculum size, and initial pH to enhance bacterial acidic agent production by *Acidithiobacillus thiooxidans*, achieving a sulfate concentration of 40.3 g/l and a ΔpH of 1.87. Metal removal efficiency was assessed at pulp densities of 10–50 g/l, demonstrating high extraction rates of Li (92%), Ni (88%), and Co (78%) at 50 g/l after 7 days. Comparative analysis with chemical leaching confirmed the effectiveness of this green strategy. Furthermore, a kinetic study using the Avrami equation and shrinking core model revealed that both models yield comparable results, and diffusion through the product layer controlled the leaching rate. This study presents a comprehensive and sustainable strategy for waste recycling at high pulp densities by integrating process optimization, spent-medium bioleaching, and kinetic modeling for critical metal extraction from lithium-ion battery cathodes.

Keywords Used lithium-ion batteries, High pulp density, Bacterial acidic agent, *Acidithiobacillus thiooxidans*, Response surface methodology, Biohydrometallurgy

Abbreviations

AI	Artificial intelligence
ANN	Artificial neural network
ANOVA	Analysis of variance
BAA	Bacterial acidic agent
CBB	Calvin–Benson–Bassham
CCD	Central composite design
DoE	Design of experiment
ICP-OES	Inductively coupled plasma-optical emission spectroscopy
IOB	Iron-oxidizing bacteria
IROST	Iranian Research Organization for Science and Technology
LIBs	Lithium-ion batteries
ML	Machine learning
RSM	Response surface methodology
RUBISCO	Ribulose-1,5-bisphosphate carboxylase/oxygenase
SA	Sulfuric acid
SC	Sulfate concentration
SD	Sulfur dosage

[1]Biotechnology Group, Chemical Engineering Department, Tarbiat Modares University, Jalal Ale Ahmad Highway, Nasr, P.O. Box 14115-111, Tehran, Iran. [2]Modares Environmental Research Institute, Tarbiat Modares University, Tehran, Iran. ✉email: mousavi_m@modares.ac.ir

SOB	Sulfur-oxidizing bacteria
ULIBs	Used LIB

Lithium-ion batteries (LIBs), renowned for their high performance, are widely used in portable electronic devices. The increasing demand for LIBs is expected to increase the number of batteries used significantly[1,2]. The stockpile of used LIBs (ULIBs) is projected to increase from approximately 0.3 million tons in 2020 to around 1.6 million tons by 2030. Properly recycling ULIBs is essential for promoting clean energy initiatives, addressing expected material shortages, and ensuring a sustainable supply of critical metals such as lithium and cobalt, whose demand is projected to exceed supply. By 2040, approximately 70% of the world's cobalt reserves will be directed toward battery production, creating an anticipated imbalance between LIB demand and raw material supply by 2030[3].

LIBs contain high concentrations of metals such as cobalt, nickel, manganese, and lithium and chemicals like electrolytes and binders, which pose significant environmental and health risks if not properly managed. Given the environmental hazards associated with ULIB disposal and the increasing demand for essential metals in LIB manufacturing, it is imperative to develop cost-effective and environmentally sustainable recycling processes[4,5].

The current techniques for recycling metals from ULIBs encompass pyrometallurgy, hydrometallurgy, and biohydrometallurgy. However, hydrometallurgy faces several challenges, including complex procedures, substantial acidic waste generation, harmful gas emissions, health and environmental risks, and costs associated with byproduct disposal. It surpasses pyrometallurgy in sustainability, extraction efficiency, energy usage, emissions, and capital expenses. Conversely, the pyrometallurgical method is less favorable due to its high energy consumption, hazardous emissions, and potential lithium loss[6–9].

Biohydrometallurgical methods, such as bioleaching, produce organic and inorganic acids by the metabolic activities of microorganisms, acting as efficient leaching agents for metals. The benefits of this strategy encompass its simplicity, cost-effectiveness, and minimal energy consumption. Although bioleaching has slower kinetics than chemical leaching, studies indicate it provides advantages over conventional methods for extracting lithium from low-grade sources[3,10]. The selection of the leaching agent depends on the type of target metals, as it plays a crucial role in enhancing metal extraction efficiency[11]. The production of these agents depends on the activity of microorganisms, including chemolithotrophic, chemoorganotrophic, and microbial consortium/mixed culture types. The primary acidophilic specializing in sulfur-oxidizing bacteria (SOB) that are utilized in the bioleaching process for extracting valuable metals from ULIBs consist of *Acidithiobacillus thiooxidans*, *Alicyclobacillus* spp., and *Sulfobacillus thermosulfidooxidans*. In the case of bioleaching for ULIBs, the predominant iron-oxidizing bacteria (IOB) employed encompass *Acidithiobacillus ferrooxidans*, *Leptospirillum ferriphilum*, and *Sulfobacillus* spp.[1,12]. They possess the ability to utilize CO_2 as their carbon source, acquiring carbon through the reductive fixation of atmospheric CO_2. Additionally, they derive energy from inorganic compounds such as ferrous ion (Fe^{2+} for IOB) and reduced sulfur (S^0 for SOB)[1,12–14].

SOB and IOB play a crucial role in metal bio-oxidation, employing two distinct mechanisms: (a) direct oxidation of the metal substrate and (b) indirect oxidation facilitated by a redox couple, exemplified by the presence of Fe^{3+} and Fe^{2+} in the metallic waste. During spent-medium bioleaching, metals are extracted from ULIBs through biogenic sulfuric acid (SA), a mechanism that encompasses proton attack and redoxolysis. As part of their metabolism, the bacterial cells convert elemental sulfur (S^0) to SA, an electron donor in the electron transport chain. The protons generated during this part of metabolism can react with the metals in ULIBs. Ferric ions act as effective oxidizing agents, amplifying the leaching reaction. Bacterial leaching involves the direct attachment of cells to the metal complexes, streamlining the acceptance of electrons from oxidized metals. Chemolithotrophic bacteria employ external elemental sulfur and ferrous ions as electron donors during bioleaching of ULIBs. The resultant biogenic SA and ferric ions facilitate the dissolution of metal ions from ULIBs[15–17]. This approach significantly expedites the re-oxidation of ferrous ions, achieving a rate approximately 10^5–10^6 times faster than chemical oxidation under pH 2–3 conditions. The bacteria promote the oxidation of elemental sulfur to sulfate, generating biogenic SA and oxidizing Fe^{2+} to Fe^{3+}[17].

Although various factors affecting the bioleaching of ULIBs have been extensively studied, microbial inhibition remains a significant challenge, particularly when pulp density increases. This issue is also observed at lower pulp densities, where a long adaptation phase is required, restricting the broader industrial application of bioleaching[18]. For instance, Roy et al.[4] investigated the enhanced recovery of Li (60%) and Co (94%) in 100 g/l pulp density by applying *A. ferrooxidans*, achieving increased SA (0.52 M) production and successfully replenishing the bacterium over three cycles. Bacterial acidic agents (BAA), including SA and other metabolites, offer a milder and more environmentally friendly alternative to commercial SA (2 M) for metal extraction[19]. In a previous study[13], a two-step bioleaching process utilizing a mixture of *A. thiooxidans* and *A. ferrooxidans* was optimized for metal extraction from ULIBs, incorporating an adaptation phase resulted in 99.2% Li, 50.4% Co, and 89.4% Ni recovery in the presence of 40 g/l pulp density. As stated earlier, this study proposes separating the acid generation step—specifically optimizing BAA production through sulfur oxidation by *A. thiooxidans*—from the metal dissolution process to overcome the associated challenges. This strategic approach, spent-medium bioleaching, presents notable advantages in mitigating biosorption and bioaccumulation issues (which resulted in three times better leaching efficiency[20]) while enabling operation at higher pulp densities. The initial stage involves cultivating and expanding the bacterial strain in a medium devoid of waste, followed by utilizing the produced metabolites for metal extraction[21]. Unlike conventional hydrometallurgical or direct bioleaching methods, spent-medium bioleaching offers key advantages for industrial application, reduced chemical consumption by replacing synthetic acids with biogenic sulfuric acid, lower environmental footprint due to minimal toxic byproduct formation, and improved scalability by mitigating biosorption and bioaccumulation issues. The spent-medium bioleaching process was suited for large-scale and requires relatively simple equipment,

such as a bioreactor, reactor, compressors, and pumps[22], offering a cost-effective and eco-friendly alternative to conventional metal recovery methods.

To achieve these objectives, this study employs an indirect green method, utilizing BAA produced by *A. thiooxidans* as a potent agent for metal extraction from ULIBs. The goal of optimizing critical parameters—including sulfur dosage (SD), inoculum size, and initial pH—via response surface methodology (RSM) is to enhance BAA production, particularly sulfate, which plays a crucial role in bioleaching efficiency. Trends in pulp density were investigated to assess metal removal efficiency across varying concentrations, and the optimal bioleaching duration was determined. The findings were then compared with chemical leaching to evaluate the efficacy of sulfate. Additionally, a kinetic study employing the shrinking core model was conducted to elucidate the rate-controlling step. The current study of indirect strategy supplies a sustainable approach for critical metal extraction from ULIBs, aligning with the high demand for green alternatives in waste management and resource recovery.

Materials and methods

ULIB powder preparation

The spent laptop batteries, consisting of 100 LIBs sourced from 20 spent laptop batteries, were purchased from a local market in Tehran, Iran. The authors adopted the same methodology for battery discharge, component separation, and ULIBs powder preparation in their previous research[13]. The particle size plays a crucial role in the dissolution of metals. Smaller particles have a higher surface/volume, enhanced the bioleaching reaction rates[23]. Optimal bioleaching conditions are typically achieved with particles smaller than 75 µm[24]. So, the electrode material was mixed, and the resultant sample was ground to a particle size of less than 75 µm using a planetary ball mill (Fritsch, Germany).

ULIB composition

The ULIB powder underwent chemical digestion using a combination of sodium–potassium carbonate, hydrochloric acid, and nitric acid. 0.25 g of ULIB powder was placed in a platinum crucible with sodium–potassium carbonate and boric acid, then heated to 950 °C in an electric furnace. After cooling, the mixture was dissolved in HCl (1:1), added to 10 ml of HNO_3–HCl in a 1:3 ratio (aqua regia), and filtered. Following appropriate dilution, the resulting solution underwent inductively coupled plasma-optical emission spectroscopy (ICP-OES, Vista-pro; Varian; Australia) analysis to determine the metallic composition of ULIB powder.

Strain cultivation and inoculum preparation

The lyophilized form of *A. thiooxidans* PTCC 1717 was purchased from the Iranian Research Organization for Science and Technology (IROST). The mineral-salt medium was prepared by dissolving 2 g of $(NH_4)_2SO_4$, 0.25 g of $K_2HPO_4{\cdot}3H_2O$, 0.25 g of $MgSO_4{\cdot}7H_2O$, and 0.1 g of KCl, along with 10 g of S^0, in 1 l of distilled water. All chemicals used in the culture medium were of analytical grade and obtained from Merck (Germany). Sulfur was added to the culture medium as the energy source for *A. thiooxidans*. The pH of the culture medium was adjusted to 2 using 98% H_2SO_4, a low pH condition favorable for the growth of *A. thiooxidans*. Due to the highly acidic condition, sterilization was unnecessary. For inoculum preparation, the strain was inoculated in 250-ml Erlenmeyer flasks containing 100 ml of the culture medium and incubated in a shaker incubator (WiseCube WIS-20; Daihan Scientific; South Korea) at 160 rpm and 32 °C. The logarithmic growth phase was attained after eight days of incubation and the resulting culture medium was used as the active bacterium inoculum for experimental runs.

Design of experiments (DoE)

Several physicochemical and biological factors can influence the bioleaching process. By employing DoE methods, a comprehensive understanding of the roles and interactions of these factors can be achieved by minimizing time, chemical, and energy consumption[25]. For this purpose, Design Expert 7.0.0 software (version 7.1.4; State-Ease, USA) was used. The three most important factors influencing the investigated process are the SD, inoculum size, and initial pH of the culture medium. Table 1 outlines the levels of these factors. The total number of experiments was determined using the formula $2^k + 2k + c$, where k represents the number of factors (in this case, $k = 3$) and c represents the number of center points set at 6. The factorial points consisted of 8 (2^3), and the axial points comprised 6 (2×3), in addition to the six center points, resulting in a total of 20 experiments conducted (Table 2).

A central composite design (CCD) based on RSM was applied to optimize two key responses: the generated sulfate concentration (SC) and ΔpH of the solution (i.e., the difference between the initial and final pH values). These responses indicate the amount of sulfur oxidation to sulfate ions by *A. thiooxidans*. First-order function mathematical models were applied to fit the responses, presenting them as a function of the parameters. If the relationship between the response and the independent variables is linear, a first-order function can be fitted

Factor	Unit	Low axial	Low factorial	Center point	High factorial	High axial
A: Sulfur dosage (SD)	(g/l)	5	7.5	10	12.5	15
B: Inoculum size	(v/v)	2	4	6	8	10
C: Initial pH	–	1	1.5	2	2.5	3

Table 1. Levels of selected factors in experimental design.

Run no.	Symbol code: factors (unit)			Responses (unit)	
	Sulfur dosage (SD) (g/l)	Inoculum size (v/v)	Initial pH	Sulfate concentration (SC) (g/l)	ΔpH
1	10	6	2	24.3	1
2	10	10	2	25.0	1.25
3	12.5	8	2.5	30.1	1.60
4	15	6	2	37.4	1.15
5	5	6	2	11.6	0.9
6	10	6	2	24.4	0.9
7	12.5	4	2.5	31.9	1.55
8	10	6	2	24.3	1
9	10	6	3	24.3	1.88
10	7.5	4	1.5	17.6	0.68
11	7.5	8	1.5	18.9	0.74
12	10	6	2	24	0.94
13	10	6	1	25.7	0.5
14	10	6	2	24.3	1
15	10	2	2	24.2	0.94
16	10	6	2	24.3	0.9
17	7.5	4	2.5	17.2	1.5
18	7.5	8	2.5	17.5	1.32
19	12.5	8	1.5	31.5	0.9
20	12.5	4	1.5	31.9	0.5

Table 2. CCD plan of factors and the results of two obtained responses.

as an approximation function for mathematical modeling. A higher-order polynomial curve can be used in a curvature mode, such as Eq. (1), which represents the second-order function or quadratic model:

$$Y = b_0 + \sum_{i=1}^{n} b_i X_i + \sum_{i=1}^{n-1} \sum_{j=1}^{n} b_{ij} X_i X_j + \sum_{i=1}^{n} b_{ii} X_i^2 + \epsilon \quad (1)$$

Y represents the response's predicted value (SC and ΔpH), n is the number of factors, and X_i and X_j are the input parameters (coded factors). Moreover, the model parameters include b_{ii} (the second-order constant), b_{ij} (the interaction coefficient), b_0 and b_i (the offset term and linear constant, respectively), and ϵ (the random error)[13].

Bioleaching experiments

BAA production based on DoE

The BAA was produced using the spent-medium method in Erlenmeyer flasks. The inoculum with a cell density of approximately 10^7 cells/ml was initially prepared, as described in "Strain cultivation and inoculum preparation" section. All experiments were conducted in 250-ml Erlenmeyer flasks containing 100 ml of salt media with varying concentrations of sulfur, as detailed in Table 2.

Before inoculation, the initial pH of each run was adjusted using 98% H_2SO_4, at the specified amount described in Table 2. The initial pH affects bacterial growth, and a significant increase in BAA production is subsequently observed. The Erlenmeyer flasks were incubated at 32 °C and 160 rpm in a shaker incubator, and after 8 days, both responses of SC and final pH of the solution were measured. The procedure for measuring SC was based on the turbidimetric method proposed by the standard operating system[26]. The software fitted mathematical models to analyze each response based on the results of the 20 runs and influential factors. Analysis of variance (ANOVA), as a statistical analysis, was performed to determine the significance of the variables. The results were used to determine the optimal parameters, which could help increase metal recovery in the later acid-leaching step by producing optimal BAA.

Leaching of ULIBs using BAA

The optimum conditions for obtaining SA were determined using RSM. Following filtration of the solution through Whatman No. 42 filter paper to obtain the cell-free medium, the centrifugation was carried out at 4 °C and 10,000 rpm for 15 min using a refrigerated centrifuge (VS-550; Vision; South Korea) to enhance separation. The bioleaching of ULIB powder was performed by combining the powder with BAA, including SA and other metabolites. However, it was crucial to investigate the optimal pulp density and bioleaching time for maximum metal extraction. 250-ml Erlenmeyer flasks containing 100 ml BAA and ULIB powder in five different pulp densities within the range of 10–50 g/l were shaken at 160 rpm and 60 °C for 7 days. The pulp density was incrementally increased, and the extraction of critical metals (Li, Co, and Ni) was measured at each pulp density (10, 20, 30, 40, and 50 g/l). The optimal pulp density was determined based on the maximum metal leaching value. In the subsequent phase, to choose the optimal processing time, solutions with the ideal BAA amounts,

and ULIB powder pulp density were subjected to bioleaching for two distinct durations, 7 and 14 days. After each bioleaching test, the metal extraction was quantified by ICP-OES analysis. The chemical leaching of metals from ULIB powder was carried out using commercial SA at an equivalent concentration to SA to explore the impact of BAA produced by *A. thiooxidans* on metal leaching. The experimental procedure was performed similarly to the bioleaching tests.

Surface morphology analysis

After the bioleaching process, the micromorphology of the ULIB powder and the bioleaching residue were examined by field emission scanning electron microscopy (FE-SEM S-4160 Hitachi, Tokyo, Japan). The solid sample was attached to sticky carbon tape and covered with a 30 nm-thick layer of gold–palladium alloy to improve the surface's electrical conductivity and create higher-resolution images.

Results and discussion

ULIB composition

The weight percentages of components are detailed, comprising 35% cathode, 30% case, 15% anode, 12% electrolyte, 5% plastic, and 3% loss. Additionally, the metal content of ULIB powder is specified as follows: 42.8% carbon, 30.4% cobalt, 10.3% lithium, 8.2% nickel, 5.2% manganese, 2.2% iron, 0.6% copper, and 0.3% aluminum[13]. The presence of carbon in the anodes is due to the availability of graphite, while the target metals—Ni, Co, and Li—are primarily located in the cathode.

Statistical analysis

Table 3 presents the results of the statistical analysis of variance for quadratic models. To predict the SC and ΔpH, full quadratic polynomial models were developed based on mathematical modeling of the responses as a function of variables. The regression analysis was performed and the models were assigned coded factors and are described in Eqs. (2) and (3).

For SC:

$$Y_{SC} = 24.26 + 6.62A + 0.066B - 0.38C - 0.47AB + 0.053AC - 0.31BC + 0.065A^2 + 0.073B^2 + 0.17C^2 \quad (2)$$

For ΔpH:

$$Y_{\Delta pH} = 0.96 + 0.051A + 0.059B + 0.37C + 0.071AB + 0.044AC - 0.074BC + 0.020A^2 + 0.038B^2 + 0.61C^2 \quad (3)$$

where Y represents the predicted values of SC and ΔpH. The offset terms in these equations have constant values of 24.26 and 0.96. Factors A, B, and C represent the SD of the culture medium, the inoculum size, and the initial pH, respectively.

The multiplication of the two factors indicates the interaction of the parameters. The positive coefficient of each factor demonstrates that the response increases with the increase of that parameter. In contrast, the negative coefficient indicates that the increment of that factor reduces the response. The statistical analysis reveals that the factor of A, which had the most substantial effect on SC, is influenced by the highest coefficient. These statistical models were subject to a significance threshold of 0.01, and p value < 0.01, with Y (Y_{SC} and $Y_{\Delta pH}$ < 0.0001), indicating that the predicted models are significant at a 99% confidence level (p value < 0.01)[27]. The lack of fit refers to comparing residual and pure errors at replicated design points. In the case of both responses, the lack

Responses	Model	ANOVA					
		Source	Sum of squares	df	Mean square	F-value	*p* value
Part A							
Sulfate concentration (SC) (g/l)	Quadratic	Model	706.30	9	78.48	940.21	< 0.0001
		Residual	0.83	10	0.083		
		Lack of fit	0.74	5	0.15	8.15	0.0190
		Pure error	0.091	5	0.018		
		Cor total	707.13	19			
ΔpH	Quadratic	Model	2.49	9	0.28	78.25	< 0.0001
		Residual	0.035	10	3.536E−003		
		Lack of fit	0.023	5	4.605E−003	1.87	0.2549
		Pure error	0.012	5	2.467E−003		
		Cor total	2.53	19			

Responses	R-squared	Adj R-squared	Adeq precision	PRESS
Part B				
Sulfate concentration (g/l)	0.9988	0.9978	129.56	6.34
ΔpH	0.9860	0.9734	35.14	0.21

Table 3. Part A: ANOVA summary of the predicted models for responses (SC and ΔpH) and Part B: ANOVA summary for fitted models applied in experimental design.

of fit was found to be 'not significant' at a p value > 0.01, which confirms the adequacy of the fitting models. The F-value shows the ratio of error variance to model variance. A high F-value indicates the importance of factors, while a value of 1 indicates that factors are insignificant. The coefficient of determination (R-squared, R^2) reflects the correlation between experimental data and the model, with R^2 values of 0.9988 for Y_{SC} and 0.9860 for $Y_{\Delta pH}$, indicating a strong correlation. The adjusted R-squared (adj R^2) is preferred over R^2, as it indicates the high significance of the model. Table 3 reports values of 0.9978 for Y_{SC} and 0.9734 for $Y_{\Delta pH}$. The results of this section demonstrated that the RSM can effectively evaluate the influence of various parameters on BSA production and determine the optimal conditions used in the bioleaching of metals in the next section. However, since bioleaching is a complex process with nonlinear relationships, more advanced modeling approaches, such as artificial intelligence (AI)-based methods, could enhance prediction accuracy while reducing the cost and time of experimental trials compared to RSM. Previous investigations have shown that machine learning (ML) and artificial neural network (ANN) can predict metal recovery rates with higher accuracy and provide a deeper understanding of the effects of key variables such as nutrition source, pulp density, particle size, temperature, and microorganism type[28,29]. Therefore, it is recommended that future studies examine integrating AI-based methods with traditional statistical approaches to develop more precise predictive models and optimize the bio-metabolites or bioleaching processes.

BAA production mechanism and results

Most acidophilic bacteria, such as *A. thiooxidans* and *A. ferrooxidans*, use the Calvin–Benson–Bassham (CBB) cycle and have the ability to fix atmospheric CO_2 for their cellular carbon requirement through the enzyme ribulose-1,5-bisphosphate carboxylase/oxygenase (RUBISCO) in this pathway. The cytoplasmic organelles in these bacteria are called carboxysomes[30]. These polyhedral organelles contain bodies produced under CO_2-limiting conditions, and RUBISCO is often packaged in them. These bacteria can increase the concentration of HCO_3 to enhance CO_2 fixation. Therefore, CO_2 is formed by carbonic anhydrase near RUBISCO, and a high concentration of the RUBISCO substrate enhances the carboxylation reaction over oxygenation[31]. *Acidithiobacillus thiooxidans* is recognized as an acidophilic strain with the ability to produce acid. It is capable of oxidizing sulfur to H_2SO_4 as well as oxidizing thiosulfate[32]. The strain mentioned shows optimal growth at a pH below 3. Acidophiles exhibit tolerance to pH gradients, denoting the difference between pH_{in} and pH_{out}. The pH gradient across the plasma membrane plays a crucial role in the cell's bioenergetics, primarily contributing to the proton motive force. Autotrophic organisms strongly require reducing their carbon source (CO_2) to compounds such as NAD(P)H, generating macromolecules such as sugars, nucleic acids, and amino acids to synthesize new cells. The hydrogen atoms resulting under acidic conditions are also essential to reduce CO_2 to cell mass produced due to a transmembrane pH gradient. In chemolithotrophic microorganisms, this large transmembrane proton gradient is necessary for energizing the synthesis of NAD(P)H and generating the needed proton motive force as reverse electron transport[33,34]. The optimization of BAA using *A. thiooxidans* was performed following the results of the 20 runs suggested by the RSM for evaluating the values of the parameters on each response, as shown in Table 2. These results were used for both model fitting and process optimization.

Response plots

Effect of factors on sulfate production

In Fig. 1a, two-dimensional contour plots were observed illustrating the influence of initial pH and SD on sulfur oxidation, with a constant inoculum size of 4% v/v. The data reveals a notable correlation between SD and sulfur oxidation, highlighting that a crucial factor in achieving effective sulfur oxidation is the direct interaction between sulfur and *A. thiooxidans*. Furthermore, the results indicate that increasing SD in the medium plays a pivotal role in enhancing bacterial activity, resulting in improved sulfur bacterial oxidation and increased sulfur consumption by the microorganism, as outlined in Eq. (4)[35–37].

$$S^0 + 1.5O_2 + H_2O \xrightarrow{\text{Bacteria}} 2H^+ + SO_4^{2-} \tag{4}$$

The periplasmic enzyme sulfur dioxygenase oxidizes elemental sulfur to sulfite and sulfate. The increase in S^0 oxidation using a wetting agent may be due to metabolites produced by the bacterium and secreted organic compounds such as amino acids, polypeptides, and phospholipids like phosphatidylinositol. The secreted proteins are involved in adhesion and are linked to electron transport, bacterial colonization, and oxidation of insoluble sulfur[33,38].

The influence of SD and inoculum size on sulfur oxidation is illustrated in the two-dimensional contour plots of Fig. 1b. As depicted in Fig. 1b, achieving maximum sulfur oxidation is possible when the SD in the culture medium exceeds 13.5 g/l, even with a smaller inoculum size and an initial pH ranging from 1 to 3. At a fixed initial pH of 2.5, the acidic conditions favor sulfate production in the medium, resulting in the highest percentage of sulfur oxidation or SC at SD above 13 g/l, regardless of the inoculum size.

However, increasing the inoculum size cannot attain the maximum percentage of sulfur oxidation at a high initial pH and low SD in the medium. This is because decreasing the S^0 content as an energy source and increasing the inoculum size reduces the adsorption of bacteria on the surface of elemental sulfur due to van der Waals forces, leading to less subsequent oxidation. Nevertheless, lower acidity is desirable from both environmental and economic perspectives because it consumes fewer chemical acids[37].

The SD in the medium must be increased to enhance the contact of bacterial cells with the sulfur surface when the inoculum size is at the lowest level of 2% v/v. Upon bacterial cell absorption onto the sulfur surface, the primary factor influencing the wetting of sulfur becomes the production of extracellular fats and protons. Conversely, augmenting the inoculum size in the culture medium leads to a greater surface area of sulfur enveloped by bacteria, thereby increasing sulfur oxidation and the SC[39].

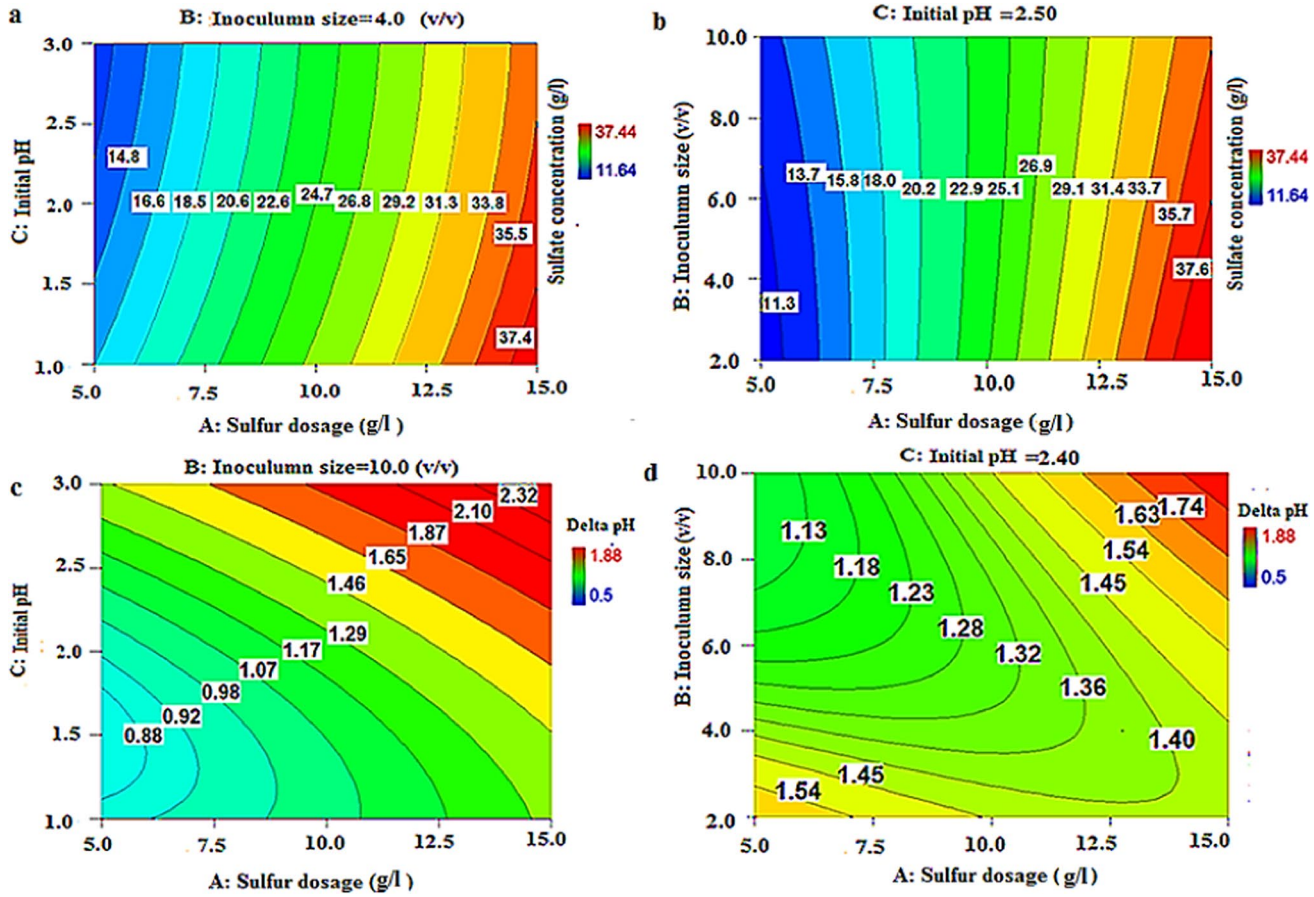

Fig. 1. Contour plots of interactions of factors for SC; (**a**) SD and initial pH at a constant inoculum size of 4% v/v, and (**b**) SD and inoculum size at a constant initial pH of 2.5. Contour plots of interactions of factors for ΔpH; (**c**) SD and initial pH at constant inoculum size of 10%v/v, and (**d**) SD and inoculum size at a constant initial pH of 2.4.

Effect of factors on ΔpH

The oxidation of sulfur can generate intermediates such as S^{2-}, $S_2O_3^{2-}$, SO_3^{2-}, and $S_4O_6^{2-}$ to satisfy the energy requirements of *A. thiooxidans*, eventually due to the production of SA. Within the bacterial cytoplasm, a sequence of catalytic reactions occurs in the intermediate metabolites of S^0, ultimately producing sulfate[40]. The production of protons resulting from BAA decreases the final pH, a mechanism known as acidolysis in the bioleaching process. High initial pH hinders microbial activity and acidophilic growth, reducing BAA production and lowering ΔpH values. The impact of the initial pH on the final pH of the medium is more significant than the other two parameters. Higher initial pH conditions are less favorable for acidophilic bacteria, resulting in decreased sulfur oxidation.

In Fig. 1c, a two-dimensional contour plot illustrates the impact of SD and initial pH on the final pH of the solution with a constant inoculum size of 10% v/v. However, increasing SD to more than 7.5 g/l allows for an acidic solution even at a higher initial pH of the medium. As previously mentioned, this is advantageous as it reduces the need for chemical acids. Research indicates that at pH < 1.0, H_2SO_4 species primarily convert to HSO_4^- (bisulfate) and H^+ (hydrogen ion) at pH < 1.0, while at pH < 3.5, a combination of bisulfate and sulfate ions is observed. At low pH, sulfate cannot function as a terminal electron acceptor due to unknown thermodynamic reasons[41]. At higher initial pH values (> 2), the bacterial and enzymatic activity of the cells and enzymatic complexation increase[32,37]. Figure 1d illustrates the relationship between inoculum size and initial sulfur concentration at a constant initial pH of 2.4. When the initial sulfur concentration is high (> 12.5 g/l), the acidic condition can be attained even at a higher initial pH and larger inoculum size (> 7% v/v), which is favorable for the acidity of the medium. It is due to increased sulfur bio-conversion, higher production of BAA, and a lower final pH in the medium. The optimization was pursued to identify the conditions for achieving the medium's highest SC and lowest final pH. The optimal condition was obtained at an initial pH of 2.71, an inoculum size of 2% (v/v), and an SD of 14.90 g/l. Under these optimum conditions, the model predicted an SC of 40.3 g/l and a ΔpH of 1.87. However, these results require to be confirmed through actual experiments. Therefore, a confirmation test was performed under the optimal conditions, and the results agreed with the predicted optimum values, as shown in Table 4.

Responses	Prediction	Confirmation test	99% CI low	99% CI high
Sulfate concentration (g/l)	40.3	39.1	38.15	42.53
ΔpH	1.87	2.19	1.42	2.32

Table 4. Verification results under optimum condition.

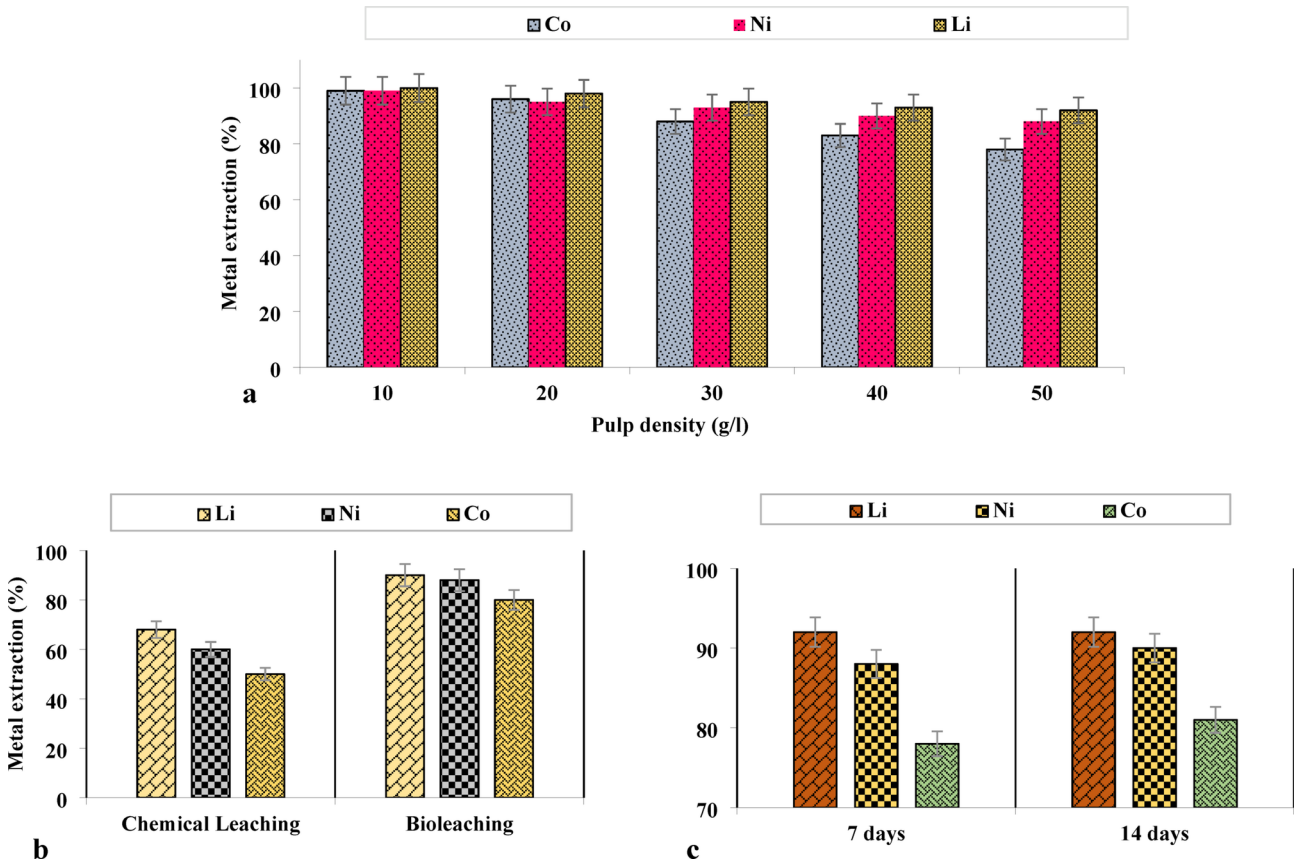

Fig. 2. (**a**) The influence of pulp density on the metal extraction of Co, Ni, and Li, (**b**) a comparison between bioleaching and chemical leaching, and (**c**) the impact of bioleaching time on metals extraction in optimum conditions.

BAA as an agent in metal extraction

The bioleaching process involves various microbial reactions that contribute to the extraction of metals from the complicated solid structure of ULIBs. Additionally, these microbial reactions transform the hazardous components of ULIBs into non-hazardous forms[42].

The mechanism of metal extraction involves a chemical process where proton ions, produced during the oxidation reaction, enhance the dissolution of metals. This process, known as protonation, is a significant mechanism in the overall bioleaching process[43]. The reduction of metallic compounds occurs through the reaction of BAA produced by bacteria, as described in Eq. (5)[37]:

$$M_2O_{x(S)} + xSO^{2-}_{4(aq)} + 2xH^{+}_{(aq)} \rightarrow M_2(SO_4)_{x(aq)} + xH_2O_{(aq)} \quad (5)$$

where M represents Li, Ni, and Co and is the metal with the valence of x in the metal oxide (M_2O_X) form[44]. $M_2(SO_4)_x$ is the leached metal by BAA ions that take the soluble form of a complex metal. The intermediate metabolites produced in the medium affect the elements with different valences. The presence of intermediate compounds like sulfite and thiosulfate is a result of a reaction mechanism involving the conversion of elemental sulfur to SA. This reaction facilitates the mobilization of metals from solid waste, and the mechanism varies based on the energy source species and metals involved[40]. The metal extraction experiment, using the BAA produced under optimal conditions, was performed at five different pulp densities ranging from 10 to 50 g/l and continued for 7 days. The metal concentrations are reported in Fig. 2a.

Total metal extraction was achieved for all three metals (Co, Ni, and Li) at a pulp density of 10 g/l. Metal extraction decreases by increasing the pulp density in the medium. Therefore, the findings for metal extraction

of Li, Co, and Ni suggested that the maximum was achieved at a pulp density of 50 g/l. Higher pulp densities are also of interest in industrial applications due to the reduction of reactor size and operational costs. In the prior study[13], metal extraction efficiencies were maximized at a pulp density of 40 g/l, with approximately 99.2% for Li, 50.4% for Co, and 89.4% for Ni under optimal conditions. This was achieved using an adapted mixed culture of *A. thiooxidans* and *A. ferrooxidans*. In the present study the highest extraction efficiency for Li, Ni, and Co were 92%, 88%, and 78%, respectively, with a pulp density increased to 50 g/l.

Extraction efficiency is strongly influenced by the agent concentration. Therefore, at a constant concentration of the culture medium's salts, increasing the pulp density reduces the amount of extraction efficiency in the control test. Consequently, based on the results of the control experiment in our previous study[13], the primary contribution to bioleaching can be attributed to the metabolites and acids produced by the microbial strain.

Despite the 10 g/l increase in pulp density in the current study, it was observed that spent-medium bioleaching using BAA proved more effective at higher pulp densities compared to the previous work, resulting in increased metal extraction. The bioleaching system in the previous study[13] involved direct bioleaching with ferric and sulfate, whereas, in the current work, exclusively sulfate produced by bacteria was utilized in spent-medium bioleaching. This approach (spent-medium bioleaching) was employed to further increase the pulp density, eliminate the extended adaptation time of the bacterium, and evaluate the effect of optimal BAA in metal extraction from ULIBs.

According to Xin et al.[15], ULIBs are composed of $LiCoO_2$ as the primary structural component, accompanied by CoO. In the SA leaching system, acidic dissolution releases Co^{2+} from CoO. Concurrently, the Co^{3+} within $LiCoO_2$, serving as the structural material, exhibits resistance to acid-induced impacts, resulting in the incomplete dissolution of Co. In contrast, Li dissolution is primarily based on acid dissolution.

Our findings align with Xin's research[15], suggesting that the recovery mechanism for Co involves a combination of acid dissolution and oxidation–reduction. The Ni extraction mechanism mirrors that of Co, entailing a combination of acid dissolution and oxidation–reduction. Both the current and previous studies demonstrate that, despite differences in leaching agents and an increase in pulp density, complete extraction of Co and Ni did not occur. This incomplete extraction can be attributed to dissolutive mechanisms, in line with Xin et al.'s findings[15]. The extraction of Li relies on an acid dissolution, with sulfur playing a crucial role in maintaining high acidity in the system. This accounts for the increased Li extraction observed in the current study compared to the previous work. Li has a high reactivity in the aqueous medium (Eq. (6)), leading to higher Li extraction in 10–50 g/l pulp densities compared to the extraction of transition metals (Ni and Co) extractions. As stated, Co and Ni in solid powder are also trivalent metals (Co^{3+} and Ni^{3+}). During bioleaching, these two metals transform to the bivalent state (Co^{2+} and Ni^{2+}) during bioleaching using a reducing agent[45].

$$4Li + 2H_2O + O_2 \rightarrow 4Li^+ + 4OH^- \tag{6}$$

Lithium is an acid-consuming metal that utilizes H^+ ions from the medium and generating hydroxyl ions according to Eq. (6). In ULIB powder, lithium exists in $LiCoO_2$ and $LiNiO_2$ forms. When subjected to the bacterial metabolite, the protons from BAA attack $LiCoO_2$, releasing lithium and cobalt, as illustrated in Eqs. (7) and (8)[19]. Furthermore, the decrease in protons during the metal leaching process leads to a reduction of Co and Ni extraction as well. Nickel is also available in its oxide form, and in this case, the protonation reaction occurs according to Eq. (9)[36].

$$4LiCoO_2 + 12H^+ \rightarrow 4Li^+ + 4Co^{2+} + 6H_2O + O_2 \tag{7}$$

$$4LiNiO_2 + 12H^+ \rightarrow 4Li^+ + 4Ni^{2+} + 6H_2O + O_2 \tag{8}$$

$$NiO + 2H^+ \rightarrow Ni^{2+} + H_2O \tag{9}$$

Figure 2b demonstrates a notable contrast between chemical leaching and bioleaching, with bioleaching proving more efficient in treating ULIBs. A longer processing time of 14 days was tested by adding BAA produced under optimal conditions to 50 g/l ULIB powder to investigate the effect of process duration on metal extraction. However, as shown in Fig. 2c, increasing the processing time from 7 to 14 days resulted in only a slight increase in metal extraction, with no change in lithium leaching. Hence, a processing time of 7 days was considered optimal and economical. The study compared the results obtained under optimal conditions with findings from various bioleaching investigations that employed bacteria and fungi. Table 5 details the microorganisms employed and the corresponding metal extraction efficiency from ULIBs. Notably, both fungi and bacteria demonstrated successful metal leaching. IOB and SOB displayed good efficiency in metal leaching. However, the BAA produced by *A. thiooxidans* in this research led to improved efficiency in the leaching of Ni, Co, and Li in higher pulp density.

Evaluation of the rate controlling step under optimal condition

A shrinking core model is a helpful tool for identifying the rate-determining step of heterogeneous solid–fluid reactions during the bioleaching of ULIBs. Five sequential steps can describe the process: (1) diffusion of reactants from the bulk solution to the fluid film surrounding the solid surface, (2) penetration of reactants into the internal layer of the solid, (3) fluid–solid chemical reaction, (4) diffusion of reaction product through the layer, and (5) diffusion of reaction product into the bulk solution[50]. The step with the lowest rate is considered the rate-controlling step. Due to the dynamic behavior and constant shaking of the flasks during the bioleaching process, the first and last steps occur quickly and are not the rate-controlling steps. Thus, among the mentioned steps, it is necessary to evaluate steps 3–5 to determine the rate-controlling step[25,51].

Microorganisms	Metal content of initial ULIBs (%w/w)	Pulp density (g/l)	Metal extraction (%)	Refs.
A. thiooxidans	Co: 15.9, Li: 2, Cu: 0.6, Mn: 0.07, and Ni: 0.038	PD: 2.5	Li: 22 and Co: 66	[42]
A. ferrooxidans	Unknown	PD:5	Li: 9 and Co: 65	[46]
A. thiooxidans	Li: 4.2 Mn: 20.5 Co: 15.6, and Ni: 15.0	PD: 10	Li: 95, Mn: 95, Co: 96, and Ni: 97	[16]
Mixed culture of *A. caldus* and *S. thermosulfidooxidans*	Li: 28.7 and Co: 35.2	PD:20	Li: 100 and Co: 99	[47]
Adapted *A. ferrooxidans* and *A. thiooxidans*	Co: 30.4, Li: 10.3, and Ni: 8.2	PD: 40	Li: 99.2, Co: 50.4, and Ni: 89.4	[13]
Bacillus foraminis	Cu: 0.11, Ni: 2.7, Li: 3.3, Co: 17.6, Mn: 24.8	PD: 10	Mn: 98, Cu: 68, Li: 41, Co: 25, and Ni: 16	[48]
Aspergillus niger	Mn: 22, Co: 17.1, Al: 9.45, Cu: 6.6, Ni: 2.8, and Li: 2.2	PD:10	Cu: 100, Li: 95, Mn: 70, Al: 65, Co: 45, and Ni: 38	[49]
A. thiooxidans	Co: 30.4, Li: 10.3, and Ni: 8.2	PD:50	Li: 92, Ni: 88, and Co: 78	This study

Table 5. The comparison of the current study with other studies.

The chemical reactions take place in a thin layer on the outer surface of the solid particle, which is not limited by product diffusion because this process occurs rapidly. This model assumes that the particle is located inside the core, which shrinks over time due to metal extraction[52]. This study also examined the Avrami equation as a model for describing heterogeneous solid–liquid reactions at an unreacted surface[53]. The kinetic study aims to determine whether the process kinetics are controlled by diffusion through the solid internal layer or chemical reactions. In the shrinking core model, an unreacted core shrinks during the process.

When the rate-controlling step is reactant diffusion through the shell of the solid and chemical reaction, the corresponding equations are Eqs. (10) and (11), respectively[54], and Eq. (12) shows the Avrami equation.

$$kt = 1 + 2(1 - x) - 3(1 - X)^{\frac{2}{3}} \tag{10}$$

$$kt = 1 - (1 - x)^{\frac{1}{3}} \tag{11}$$

$$\ln k + n \ln t = \ln[-\ln(1 - x)] \tag{12}$$

where x represents the leaching efficiency, k denotes the reaction rate constant (min^{-1}), *t* stands for the reaction time (min), and n is a suitable parameter. However, Eqs. (10) and (11) assume a constant concentration of the leaching agent (sulfate in this study), which is far from reality. Therefore, Eqs. (13) and (14) can be used to describe the mechanism of the shrinking core model. Equation (13) describes the diffusion control process, while Eq. (14) describes the chemical reaction control process[25,50].

$$E(x) = 1 - 2/3x(t) - (1 - x(t))^{2/3} = \frac{2bD_e}{\rho_X R^2 (1 - \epsilon)} \int_0^t C_{sulfat} dt \tag{13}$$

$$G(x) = 1 - (1 - x(t))^{1/3} = \frac{bk^*}{\rho_X R(1 - \epsilon)} \int_0^t C_{sulfate} dt \tag{14}$$

The molar density of elements in ULIB is denoted as ρ_X, where C represents the sulfate ion concentration, De is the diffusion coefficient of sulfate, R is the solid particle radius, and ε is the particle porosity. The term $\int_0^t C_{sulfate} dt$ is regarded as a function of time[50].

Bioleaching was performed with BAA produced under optimal conditions and 50 g/l of ULIB powder, with daily sample collection for the kinetic study. SC and metal extraction were measured for each sample. Two kinetic models, the modified or E(x) model and the conventional or G(x) model, were fitted to $\int_0^t C_{sulfate} dt$. The line that best fits the experimental data indicates the rate-controlling mechanism. The results of the model fitting were illustrated in Fig. 3a–i. It is evident that, for all metals, the modified model that considers the variation in SC over time fits the data better than the conventional model, which ignores such variation. A comparison of the R^2 values derived from fitting the experimental data to the equations of diffusion control and chemical reaction control reveals that, for all three metals (Li, Ni, and Co), the diffusion control model provides a better fit to the data, with higher R^2 values of approximately 0.8062, 0.8045, and 0.8038, respectively. On the other hand, the kinetic analyses of the experimental data using the Avrami equation revealed R^2 of 0.7738 for Co, 0.7761 for Ni, and 0.864 for Li in the bioleaching process.

It suggests that the rate-controlling step for metal extraction is the diffusion through the solid layer, owing to the low porosity of solid particles[27,55]. Time and operating costs play a key role in the industrialization of this process. Based on the data from this study, the reaction kinetics have shown that the rate-controlling step is diffusion. This indicates that it is not enough to increase the concentration of chemical reagents; it is also necessary to investigate the factors that decrease diffusion in bioreactors and on larger scales.

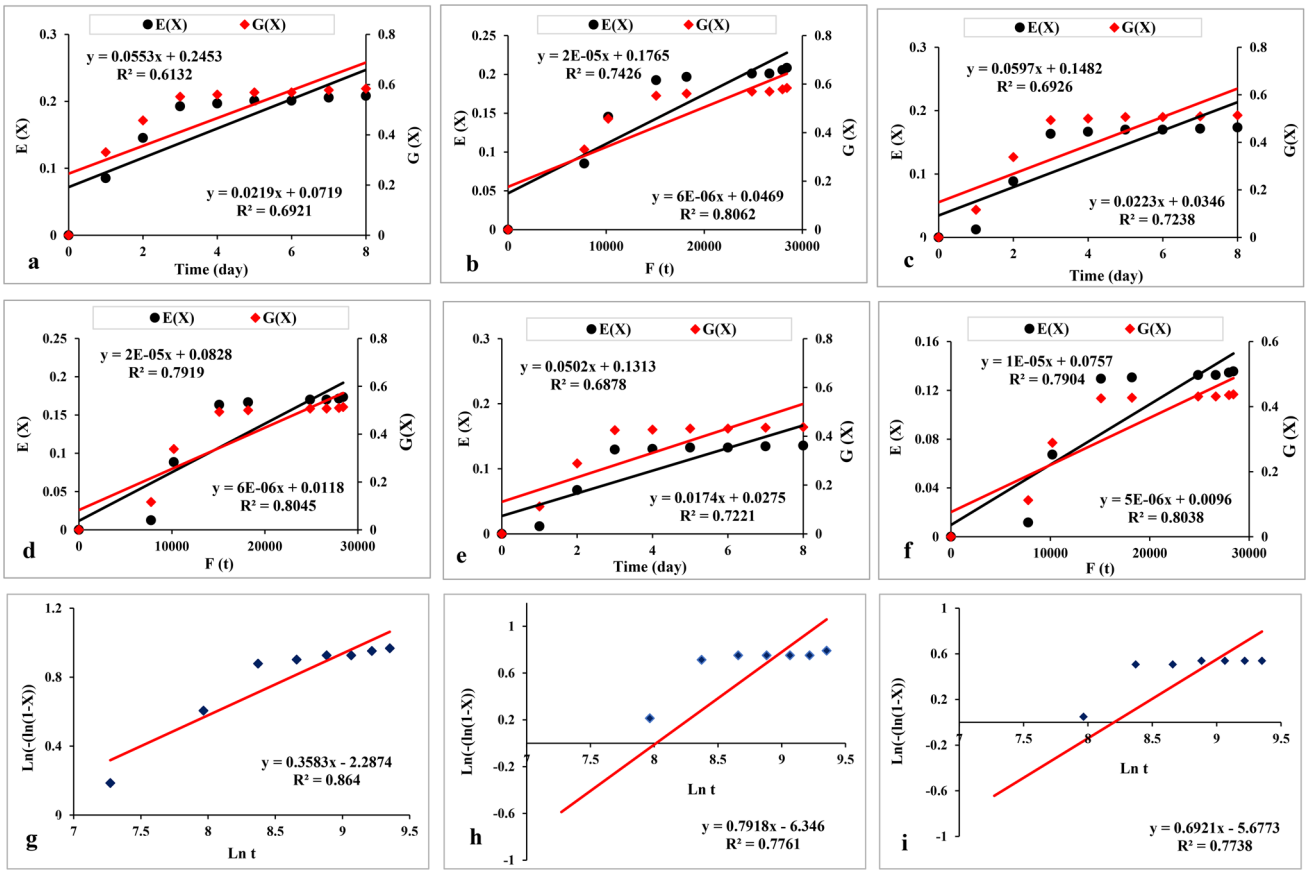

Fig. 3. Model fitting to experimental data by shrinking core model; (**a**) conventional model for lithium; (**b**) modified model for lithium; (**c**) conventional model for nickel; (**d**) modified model for nickel; (**e**) conventional model for cobalt; and (**f**) modified model for cobalt; and Avrami equation for; (**g**) lithium; (**h**) nickel; (**i**) cobalt.

Therefore, optimizing the process parameters to balance bioleaching time and costs is vital to maintain the efficiency of recovery on an industrial scale. SEM analysis described in the next section ("Surface morphology of ULIB powder" section), further supports the observation of this low porosity.

Surface morphology of ULIB powder

Figure 4a and b presents the morphology of the ULIB sample and the bioleaching residue. The SEM images reveal a significant difference in the surface morphology of the two samples, indicating the effect of the acidic medium, redox reactions, and metabolites produced by acidophilic bacteria on the surface of the waste[27,56].

The smaller particles of ULIB powder seen in Fig. 4b are believed to have formed due to metal mobilization during bioleaching. Before bioleaching, the surface of the ULIB sample appeared smooth (Fig. 4a). In contrast, a rougher and more uneven surface was observed after bioleaching, as seen in the different magnifications of Fig. 4b.

Conclusion

This study extensively explored the effectiveness of BAA produced by *A. thiooxidans* in extracting Li, Ni, and Co from ULIB powder. The primary focus was developing an indirect green hydrometallurgical process for metal leaching from ULIBs, emphasizing parameter optimization through RSM. The investigation considered variations in SD, inoculum size, and initial pH within the spent-medium bioleaching process, considering the escalating trend in powder pulp density for precise metal removal evaluation. Results showed that an SD of 14.90 g/l, inoculum size of 2% v/v, and initial pH of 2.7 significantly increased sulfate production to 40.3 g/l, reducing pH to 1.87. Metal removal efficiency was rigorously assessed across pulp densities (10–50 g/l), revealing extraction efficiency of 92%, 88%, and 78% for Li, Ni, and Co after 7 days at 50 g/l of powder. The results obtained from the shrinking core model closely matched those of the Avrami equation, indicating the diffusion control mechanism's superior alignment with experimental data. This emphasizes the significance of leaching agent diffusion into the solid core layer as the rate-controlling step. SEM analysis affirmed the efficacy of bacterial activity in bioleaching, surpassing chemical leaching in treating ULIBs. *Acidithiobacillus thiooxidans* for bioleaching offers a promising technology to mitigate environmental hazards associated with this waste. Findings suggest bioleaching as a direct and feasible option for large-scale industrial applications without requiring strain adaptation for managing hazardous waste.

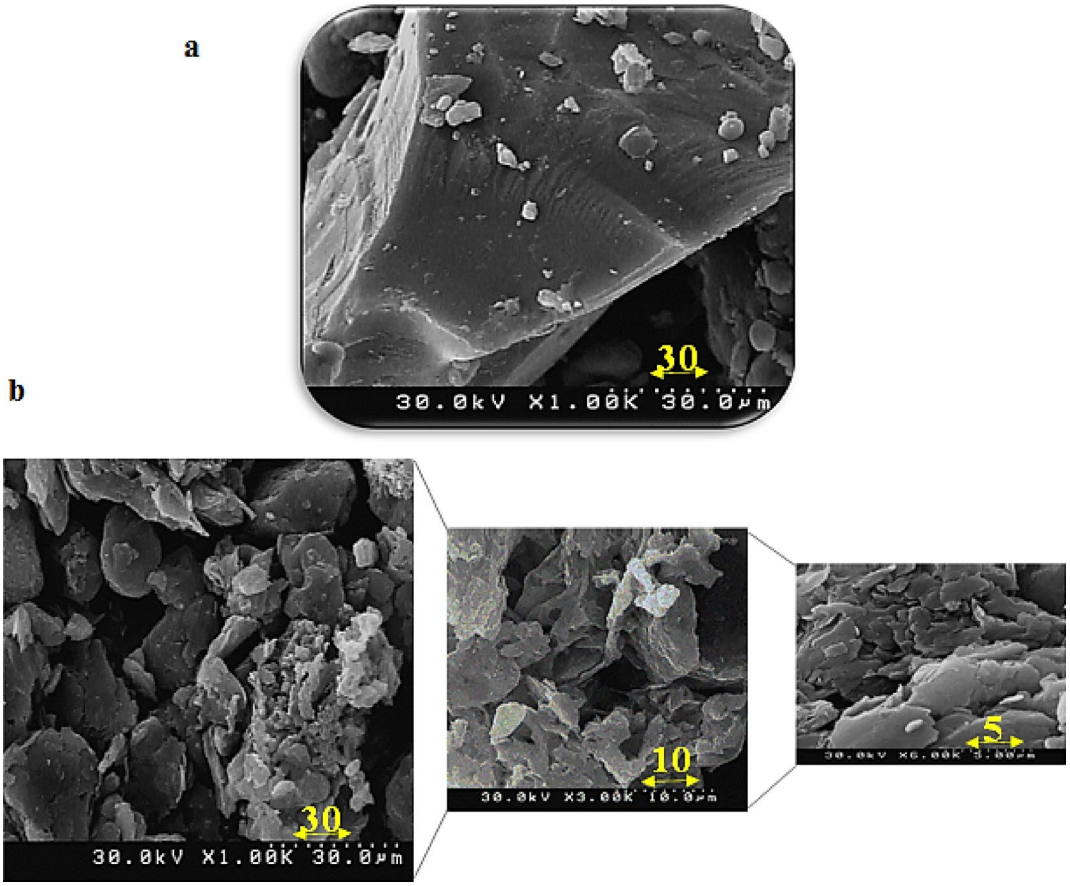

Fig. 4. FE-SEM images of ULIB; (**a**) before and (**b**) after the bioleaching process at different magnitudes.

Data availability

The datasets used and analyzed during the current study available from the corresponding author on reasonable request.

Received: 5 February 2025; Accepted: 29 April 2025
Published online: 13 May 2025

References

1. Biswal, B. K. & Balasubramanian, R. Recovery of valuable metals from spent lithium-ion batteries using microbial agents for bioleaching: A review. *Front. Microbiol.* **14**, 1–25 (2023).
2. Srichandan, H., Mohapatra, R. K., Parhi, P. K. & Mishra, S. Bioleaching approach for extraction of metal values from secondary solid wastes: A critical review. *Hydrometallurgy* **189**, 105122 (2019).
3. Alipanah, M., Reed, D., Thompson, V., Fujita, Y. & Jin, H. Sustainable bioleaching of lithium-ion batteries for critical materials recovery. *J. Clean. Prod.* **382**, 135274 (2023).
4. Roy, J. J., Madhavi, S. & Cao, B. Metal extraction from spent lithium-ion batteries (LIBs) at high pulp density by environmentally friendly bioleaching process. *J. Clean. Prod.* **280**, 124242 (2021).
5. Chernyaev, A., Zhang, J., Seisko, S., Louhi-Kultanen, M. & Lundström, M. Fe^{3+} and Al^{3+} removal by phosphate and hydroxide precipitation from synthetic NMC Li-ion battery leach solution. *Sci. Rep.* **13**, 21445 (2023).
6. Miao, Y., Liu, L., Zhang, Y., Tan, Q. & Li, J. An overview of global power lithium-ion batteries and associated critical metal recycling. *J. Hazard. Mater.* **425**, 127900 (2022).
7. Vakilchap, F., Mousavi, S. M., Baniasadi, M. & Farnaud, S. Development and evolution of biocyanidation in metal recovery from solid waste: A review. *Rev. Environ. Sci. Bio Technol.* **19**, 509–530 (2020).
8. Sedlakova-Kadukova, J. et al. Comparison of three different bioleaching systems for Li recovery from lepidolite. *Sci. Rep.* **10**, 14594 (2020).
9. Chen, M. et al. Closed loop recycling of electric vehicle batteries to enable ultra-high quality cathode powder. *Sci. Rep.* **9**, 1654 (2019).
10. Ghassa, S., Farzanegan, A., Gharabaghi, M. & Abdollahi, H. Novel bioleaching of waste lithium ion batteries by mixed moderate thermophilic microorganisms, using iron scrap as energy source and reducing agent. *Hydrometallurgy* **197**, 105465 (2020).
11. Barrueto, Y., Hernández, P., Jiménez, Y. P. & Morales, J. Properties and application of ionic liquids in leaching base/precious metals from e-waste. A review. *Hydrometallurgy* **212**, 105895 (2022).
12. Huang, T., Liu, L. & Zhang, S. Recovery of cobalt, lithium, and manganese from the cathode active materials of spent lithium-ion batteries in a bio-electro-hydrometallurgical process. *Hydrometallurgy* **188**, 101–111 (2019).
13. Heydarian, A., Mousavi, S. M., Vakilchap, F. & Baniasadi, M. Application of a mixed culture of adapted acidophilic bacteria in two-step bioleaching of spent lithium-ion laptop batteries. *J. Power Sources* **378**, 19–30 (2018).

14. Faraji, F., Golmohammadzadeh, R., Rashchi, F. & Alimardani, N. Fungal bioleaching of WPCBs using *Aspergillus niger*: Observation, optimization and kinetics. *J. Environ. Manag.* **217**, 775–787 (2018).
15. Xin, B. et al. Bioleaching mechanism of Co and Li from spent lithium-ion battery by the mixed culture of acidophilic sulfur-oxidizing and iron-oxidizing bacteria. *Bioresour. Technol.* **100**, 6163–6169 (2009).
16. Xin, Y. et al. Bioleaching of valuable metals Li Co, Ni and Mn from spent electric vehicle Li-ion batteries for the purpose of recovery. *J. Clean. Prod.* **116**, 249–258 (2016).
17. Roy, J. J., Cao, B. & Madhavi, S. A review on the recycling of spent lithium-ion batteries (LIBs) by the bioleaching approach. *Chemosphere* **282**, 130944 (2021).
18. Maluleke, M. D., Kotsiopoulos, A., Govender-Opitz, E. & Harrison, S. T. L. Microbial immobilisation and adaptation to Cu^{2+} enhances microbial Fe^{2+} oxidation for bioleaching of printed circuit boards in the presence of mixed metal ions. *Res. Microbiol.* **175**, 104148 (2024).
19. Takacova, Z., Havlik, T., Kukurugya, F. & Orac, D. Cobalt and lithium recovery from active mass of spent Li-ion batteries: Theoretical and experimental approach. *Hydrometallurgy* **163**, 9–17 (2016).
20. Natarajan, G. & Ting, Y. Gold biorecovery from e-waste: An improved strategy through spent medium leaching with pH modification. *Chemosphere* **136**, 232–238 (2015).
21. Dalini, E. A., Karimi, G. & Zandevakili, S. Treatment of valuable metals from leaching solution of spent lithium-ion batteries. *Miner. Eng.* **173**, 107226 (2021).
22. Van Yken, J. et al. Potential of metals leaching from printed circuit boards with biological and chemical lixiviants. *Hydrometallurgy* **196**, 105433 (2020).
23. Hong, M. et al. A review on bornite (bio)leaching. *Miner. Eng.* **174**, 107245 (2021).
24. Rouchalova, D., Rouchalova, K., Janakova, I., Cablik, V. & Janstova, S. Bioleaching of iron, copper, lead, and zinc from the sludge mining sediment at different particle sizes, pH, and pulp density using *Acidithiobacillus ferrooxidans*. *Minerals* **10**, 1013 (2020).
25. Motaghed, M., Mousavi, S. M., Rastegar, S. O. & Shojaosadati, S. A. Bioresource technology platinum and rhenium extraction from a spent refinery catalyst using *Bacillus megaterium* as a cyanogenic bacterium : Statistical modeling and process optimization. *Bioresour. Technol.* **171**, 401–409 (2014).
26. Rossum, J. R. & Villarruz, P. A. Suggested method for turbidimetric determination of sulfate in water. *J. Am. Water Works Assoc.* **53**, 873–876 (1961).
27. Rasoulnia, P. & Mousavi, S. M. Maximization of organic acids production by *Aspergillus niger* in a bubble column bioreactor for V and Ni recovery enhancement from power plant residual ash in spent-medium bioleaching experiments. *Bioresour. Technol.* **216**, 729–736 (2016).
28. Vyas, S., Das, S. & Ting, Y. P. Predictive modeling and response analysis of spent catalyst bioleaching using artificial neural network. *Bioresour. Technol. Rep.* **9**, 100389 (2020).
29. Mokarian, P. et al. The advanced design of bioleaching process for metal recovery: A machine learning approach. *Sep. Purif. Technol.* **291**, 120919 (2022).
30. Federici, F., Orsi, E. & Nikel, P. I. From rags to riches: Exploiting the Calvin–Benson–Bassham cycle for biomanufacturing. *ChemCatChem* **15**, 161–197 (2023).
31. Barrie Johnson, D. & Hallberg, K. B. Carbon, iron and sulfur metabolism in acidophilic micro-organisms. In *Advances in Microbial Physiology*, vol. 54 (2008).
32. Lata, S., Sharma, S. & Kaur, S. Bioleaching and biosorption of waste: Approaches and utilization. *Bio-Based Mater. Waste Energy Gener. Resour. Manag.* **106**, 331–355 (2023).
33. Bobadilla Fazzini, R. A., Levican, G. & Parada, P. *Acidithiobacillus thiooxidans* secretome containing a newly described lipoprotein Licanantase enhances chalcopyrite bioleaching rate. *Appl. Microbiol. Biotechnol.* **89**, 771–780 (2011).
34. Lin, J., Chen, L. X. & Lin, J. Acidophiles—Fundamentals and applications. In *Acidophiles—Fundamentals and Applications*. https://doi.org/10.5772/intechopen.87574 (2021).
35. Kremser, K. et al. Optimized biogenic sulfuric acid production and application in the treatment of waste incineration residues. *Waste Manag.* **144**, 182–190 (2022).
36. Yin, H. et al. Whole-genome sequencing reveals novel insights into sulfur oxidation in the extremophile *Acidithiobacillus thiooxidans*. *BMC Microbiol.* **14**, 1–14 (2014).
37. Rastegar, S. O., Mousavi, S. M., Shojaosadati, S. A. & Gu, T. Bioleaching of fuel-oil ash using *Acidithiobacillus thiooxidans* in shake flasks and a slurry bubble column bioreactor. *RSC Adv.* **6**, 21756–21764 (2016).
38. Inaba, Y., Kernan, T., West, A. C. & Banta, S. Dispersion of sulfur creates a valuable new growth medium formulation that enables earlier sulfur oxidation in relation to iron oxidation in *Acidithiobacillus ferrooxidans* cultures. *Biotechnol. Bioeng.* **118**, 3225–3238 (2021).
39. Ishigaki, T., Nakanishi, A., Tateda, M., Ike, M. & Fujita, M. Bioleaching of metal from municipal waste incineration fly ash using a mixed culture of sulfur-oxidizing and iron-oxidizing bacteria. *Chemosphere* **60**, 1087–1094 (2005).
40. Shahrabi-Farahani, M., Yaghmaei, S., Mousavi, S. M. & Amiri, F. Bioleaching of heavy metals from a petroleum spent catalyst using *Acidithiobacillus thiooxidans* in a slurry bubble column bioreactor. *Sep. Purif. Technol.* **132**, 41–49 (2014).
41. Saidan, M., Brown, B. & Valix, M. Leaching of electronic waste using biometabolised acids. *Chin. J. Chem. Eng.* **20**, 530–534 (2012).
42. Biswal, B. K. et al. Biological leaching and chemical precipitation methods for recovery of Co and Li from spent lithium-ion batteries. *ACS Sustain. Chem. Eng.* **6**, 12343–12352 (2018).
43. Gerayeli, F., Ghojavand, F., Mousavi, S. M., Yaghmaei, S. & Amiri, F. Screening and optimization of effective parameters in biological extraction of heavy metals from refinery spent catalysts using a thermophilic bacterium. *Sep. Purif. Technol.* **118**, 151–161 (2013).
44. Liu, H. L., Chen, B. Y., Lan, Y. W. & Cheng, Y. C. Biosorption of Zn(II) and Cu(II) by the indigenous *Thiobacillus thiooxidans*. *Chem. Eng. J.* **97**, 195–201 (2004).
45. Meshram, P., Pandey, B. D. & Mankhand, T. R. Recovery of valuable metals from cathodic active material of spent lithium ion batteries: Leaching and kinetic aspects. *Waste Manag.* **45**, 306–313 (2015).
46. Mishra, D., Kim, D. J., Ralph, D. E., Ahn, J. G. & Rhee, Y. H. Bioleaching of metals from spent lithium ion secondary batteries using *Acidithiobacillus ferrooxidans*. *Waste Manag.* **28**, 333–338 (2008).
47. Liao, X. et al. Feasibility of reduced iron species for promoting Li and Co recovery from spent $LiCoO_2$ batteries using a mixed-culture bioleaching process. *Sci. Total Environ.* **830**, 154577 (2022).
48. Sadeghi, N., Vakilchap, F., Ilkhani, Z. & Mousavi, S. M. Assessment of the visible light effect on one-step bacterial leaching of metals from spent lithium-ion batteries cathode pretreated by a bio-chemical lixiviant. *J. Clean. Prod.* **436**, 140432 (2024).
49. Horeh, N. B., Mousavi, S. M. & Shojaosadati, S. A. Bioleaching of valuable metals from spent lithium-ion mobile phone batteries using *Aspergillus niger*. *J. Power Sources* **320**, 257–266 (2016).
50. Jowkar, M. J., Bahaloo-Horeh, N., Mousavi, S. M. & Pourhossein, F. Bioleaching of indium from discarded liquid crystal displays. *J. Clean. Prod.* **180**, 417–429 (2018).
51. Saldaña, M. et al. Bioleaching modeling—A review. *Materials (Basel)* **16**, 3812 (2023).
52. Yang, Y. et al. Bioleaching waste printed circuit boards by *Acidithiobacillus ferrooxidans* and its kinetics aspect. *J. Biotechnol.* **173**, 24–30 (2014).
53. Fan, E. et al. Glucose oxidase-based biocatalytic acid-leaching process for recovering valuable metals from spent lithium-ion batteries. *Waste Manag.* **114**, 166–173 (2020).
54. Abdollahi, H. et al. Bioleaching of cobalt from magnetite-rich cobaltite-bearing ore. *Hydrometallurgy* **204**, 105727 (2021).

55. Amiri, F., Mousavi, S. M., Yaghmaei, S. & Barati, M. Bioleaching kinetics of a spent refinery catalyst using *Aspergillus niger* at optimal conditions. *Biochem. Eng. J.* **67**, 208–217 (2012).
56. Vakilchap, F. & Mousavi, S. M. Structural study and metal speciation assessments of waste PCBs and environmental implications: Outlooks for choosing efficient recycling routes. *Waste Manag.* **151**, 181–194 (2022).

Author contributions

A.H. conducted experiments and curated data. F.V. analyzed data and wrote the draft manuscript and also revised it. S.N.M. Analyzed data, reviewed and edited the draft, and revised the manuscript. S.M.M. supervised the research, analyzed data, reviewed and edited the draft and revised version.

Declarations

Competing interests

The authors declare no competing interests.

Additional information

Correspondence and requests for materials should be addressed to S.M.M.

Reprints and permissions information is available at www.nature.com/reprints.

Publisher's note Springer Nature remains neutral with regard to jurisdictional claims in published maps and institutional affiliations.